Coaxial Termination Load for High-Voltage Fast Transient Pulse Measurement

Seung-Kab Ryu and Yong-Hoon Kim, *Member, IEEE*

***Abstract*—A high-voltage fast transient pulse termination load using a 10-mm distributed ceramic-carbon-rod resistor has been developed. It is capable of measuring a pulse's voltage amplitudes up to 100 kV and a rise time less than 300 ps. A difficulty for the development of the high-voltage ultrawideband (UWB) termination device is the compromise of the resistive element size considering opposite characteristics of the high voltage and the wideband frequency. A smaller resistor shows the better high-frequency performance but the worse high-voltage insulation characteristic. Many previous studies in the area of pulsed-power development have used a nonscaled load device for the pulse termination; nevertheless, a mismatch between a source and a load impedance results in significant misunderstanding of the output voltage in a high-voltage fast transient pulse measurement. In this paper, we propose a newly developed high-voltage UWB coaxial load improving impedance characteristics of a nonscaled load device. Physical length of a rod resistor is far longer than a wavelength of an input pulse so that the impedance linearly increases in the moving direction of the incoming pulse. The proposed log-scaled coaxial load device with a distributed ceramic-carbon-rod resistor has a property of compensating impedance variations, which is caused by the usage of an electrically long rod resistor, by means of diminishing coaxial characteristic impedance exponentially along the resistor. This diminishing coaxial structure makes it possible to maintain consistent impedance through the entire load device. Experimental results show good agreement with expectations in aspects of the voltage standing-wave ratio under 1.25 : 1 from dc to 10 GHz; peak impedance variations under 10% with the final converged impedance of 54.86 Ω; and negligible reflections when injecting the repetitive pulsed input with amplitudes from 15 to 100 kV, a rise time below 300 ps, and repetition rates under 10 kHz.**

***Index Terms*—Distributed rod resistor, high-voltage fast transient pulse termination, ultrawideband (UWB) coaxial load.**

I. Introduction

MEASUREMENT of a high-voltage fast transient pulse has received considerable attention in many fields such as high-power vulnerability studies on information and communication electronic equipment pieces in electromagnetic (EM) compatibility area [1]–[5], a dielectric surface treatment and a modification in the material science area [6]–[8], and a noninvasive cell manipulation experiment in the biomedical area [9], [10]. An important instrument for measuring such a high-voltage fast transient pulse is the load device, as well as a voltage signal probe or a pulse-attenuating device [1]. For the high-voltage ultrawideband (UWB) pulse termination load, a fast response time with a wide frequency bandwidth and a high insulation property should be simultaneously achieved. Many investigations relating developments of a sub- or a nanosecond range pulsed-power source have been carried out. Results of the output amplitude and rise times were obtained using a capacitive voltage divider (CVD) with a matched load [11]–[16]. However, the termination load device does not seem to have a broadband frequency performance enough to measure the output pulse having a rise time less than 100–300-ps range because none of the matched resistors are small enough to function as a component with lumped parameters at voltage greater than tens of kilovolts. For this reason alone, good matching is practically unattainable [12]–[15]. When the impedance of the load is not matched, results of output voltage amplitude can be seriously misunderstood, which could be read as doubled values than the real one. In [11], an oil-filled load device was used with a CVD for testing the impulse amplitudes up to 160 kV with a rise time of 180 ps. It was composed of an oil-filled transmission line and a noninductive 45-Ω bulk resistor. The insulation and frequency performance could be achieved partially in the low-frequency region, but the high frequency matching performance would be poor due to the distributed characteristics of the bulk resistor. It might be also troublesome due to additional considerations of filling the oil and preventing oil leakages. Spikings had shown a tapered coaxial load-type attenuator that has a similar structure with this paper [17]. However, the input side of a conjunction face between a cable center line and a transition electrode might show poor impedance performance due to the integrating structure. A breakdown could be also occurred, even using the oil around the center line, since the breakdown happens along the surface of dielectrics. For operating at higher voltage levels, the input structure should be changed, as described in this paper. Barth Electronics Inc. is famous for products of high-voltage fast transient diagnostics. It produces many types of attenuators, connectors, terminators, and so on. However, the termination products have the limit of operation voltages up to 10 kV. For extending the voltage levels up to 100 kV, the insulation and impedance matching structure should be changed to avoid a breakdown at the input side.

Manuscript received January 12, 2012; revised July 12, 2012 and September 27, 2012; accepted October 24, 2012. Date of publication February 24, 2013; date of current version March 7, 2013. This work was supported in part by the Korea Communications Commission and in part by the BK21 Program at Gwangju Institute of Science and Technology.

S.-K. Ryu is with the Convergence Technology Department, Attached Institute of Electronics and Telecommunication Research Institute, Daejeon 305-600, Korea, and also with the Department of Mechatronics, Gwangju Institute of Science and Technology, Gwangju 500-712, Korea (e-mail: skryu@ensec.re.kr).

Y.-H. Kim is with the Department of Mechatronics, Gwangju Institute of Science and Technology, Gwangju 500-712, Korea (e-mail: yhkim@gist.ac.kr).

Color versions of one or more of the figures in this paper are available online at http://ieeexplore.ieee.org.

Digital Object Identifier 10.1109/TPS.2012.2234482

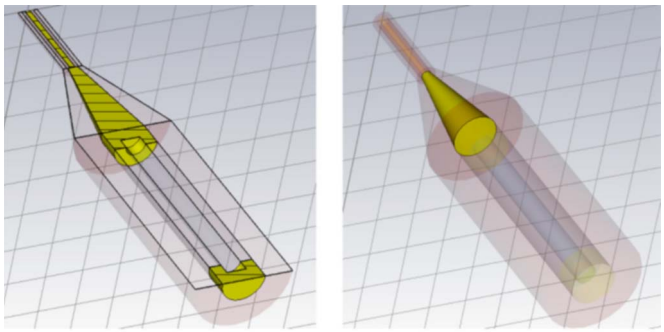

(a) (b)

Fig. 1. Structure for the nonscaled high-voltage coaxial termination load: (a) cross-sectional view and (b) assembly view.

In this paper, we propose the log-scaled coaxial load for terminating the high-voltage UWB pulse signal using a distributed ceramic-carbon-rod resistor without any insulation oils or gases. The proposed load device has an exponentially diminishing dielectric structure compensating impedance variations due to the usage of the distributed rod resistor. The aim of this paper is to develop a coaxial 50-Ω termination load handling pulse voltages up to 100 kV, full-width at half-maximum (FWHM) amplitude in 2–10-ns range, a rise time below 1 ns, and repetition frequencies below 10 kHz. Static EM analysis of the impedance matching at all of the interfaces is performed using CST Microwave Studio. Results of EM analysis would give an intuitive understanding of the design for the high-voltage UWB pulse termination load.

This paper is organized as follows. Section II covers operation principles of a high-voltage UWB coaxial termination load adopting a distributed resistive element of a tube- or rod-type carbon resistor. We introduce two cases showing different characteristics of the coaxial impedance. One is a case of no transformation in coaxial structures of enclosing dielectric's diameter. This structure is called with a nonscaled coaxial structure. The other one is a case of changing dielectric's diameter exponentially. We call this structure with the log-scaled coaxial structure. In Section III, the coaxial load structure is described in detail with simple formulas to calculate the coaxial characteristic impedance. We show some simulation results relating load performances in time and frequency domains using CST Microwave Studio. Connectors and adaptors for an interface of the high-voltage pulsed-power sources having amplitudes up to 100 kV with a rise time below 300 ps are also presented. In Section IV, the experimental setup and techniques are represented, including a Marx-driven high-voltage UWB pulse generator and a capacitive voltage pulse divider. Measurement results will be described and discussed in Section V. Finally, Section VI will draw summaries and conclusions.

II. Operation Principle of the Proposed Structure

A. Nonscaled Coaxial Structure

A nonscaled coaxial structure for the load device is shown in Fig. 1. Thickness of a center conductor at the transition from a feeding cable to a contacting electrode of a resistor is linearly increased in order to use a solid rod-type carbon resistor of which the diameter is 10 mm. In the nonscaled structure, characteristic impedance of the coaxial line does not need to be changed. Many previous works used this structure [12]–[15], but it imposes open impedance characteristics as the frequency of the input pulse goes higher. A problem when using such a nonscaled load device with a CVD for measuring the high-voltage fast transient pulses is that results could contain errors in measured voltage levels differing from the real values. It is because termination impedance is much greater than the source impedance in the high-frequency region. The nonscaled coaxial termination load was implemented to verify the theorem above and is shown in Fig. 2. A carbon resistor was used as a center conductor, of which the diameter and length are 10 and 100 mm, respectively. We used CST Microwave Studio for a small-signal analysis and modeled the ceramic carbon resistor having uniformly distributed sheet resistance on a specific cylindrical volume. Simulated frequency response was well coincident with the expectation that shows −10 dB return loss just below 100 MHz. If the front of a pulse rises within 3–4 ns, the device no more operates as a termination load. Fig. 3 describes results of the time-domain reflectometry (TDR). Reflected pulses are appeared on 650 ps, which denote the junction between the input electrode and the carbon resistor. Reflection ratio is about 40%. It implies that a nonscaled structure cannot be a good device for terminating a high-voltage wideband pulse signal.

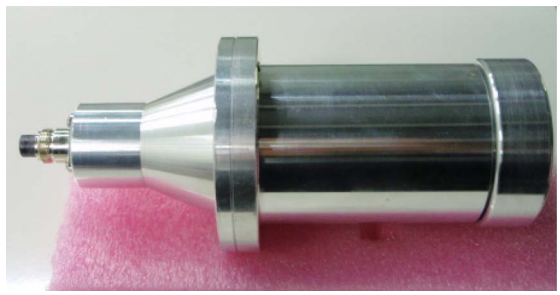

Fig. 2. Photograph of the implemented nonscaled coaxial load device.

B. Log-Scaled Coaxial Structure

In this paper, we propose a log-scaled coaxial structure for compensating impedance variations, which is caused by the usage of a distributed carbon resistor, by means of decreasing coaxial characteristic impedance linearly along the direction of an incoming pulse.

Fig. 4 represents an operation principle of the log-scaled coaxial load. When a short pulse travels an electrically long resistor, it does not operate as a lumped element. Due to the distributed characteristics, the synthetic coaxial impedance is varied at every position. If a volume resistor has a linear characteristic with respect to its physical length, it can be modeled as the uniformly distributed resistive material. The impedance would be increased from 0 to 50 Ω linearly.

The impedance mismatching problem could be solved by changing the coaxial characteristic impedance in accordance with the impedance variation due to the inserted rod resistor

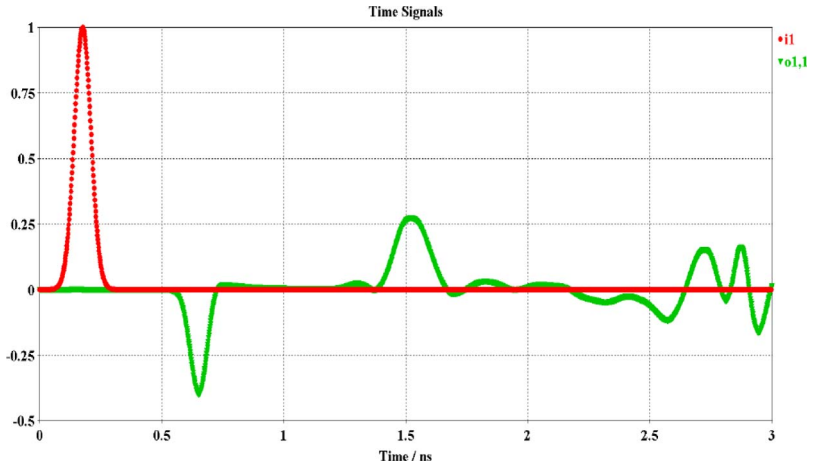

Fig. 3. Reflection diagram of a nonscaled coaxial load device: (a) incident pulse waveform (dotted line) and (b) reflected pulse waveform (solid line).

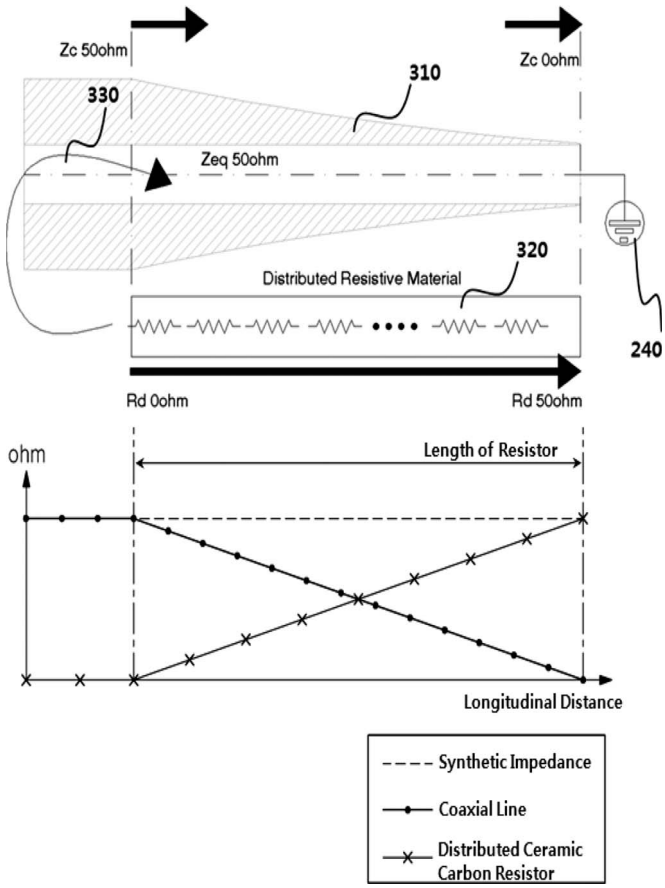

Fig. 4. Operation principle of a log-scaled coaxial termination load.

along the longitudinal direction. In Fig. 4, the resistance of the distributed ceramic-carbon-rod resistor varies from 0 to 50 Ω linearly in the step of 0.5 Ω/mm. The physical length of the resistor is 100-mm long. Conversely, the characteristic impedance of the coaxial line is linearly decreasing from 50 to 0 Ω with the same rate of the impedance variations caused by the rod resistor. Thus, the synthetic impedance of the log-scaled coaxial load device can be maintained with 50 Ω consistently over the entire load structure along the propagation path of an incoming pulse.

III. Design of the Log-Scaled Coaxial Load Device With a Distributed Ceramic-Carbon-Rod Resistor

A. Distributed Resistor Model

A commercial ceramic-carbon-rod resistor (diameter of 10 mm, length of 100 mm) is considered for the center conductor in the coaxial line. As the operation frequency goes higher, a current will flow along a surface of the material so that a volume resistor can be modeled having sheet resistance. Although the resistance distribution property is strongly dependent on a manufacturing process of the carbon resistor, we assumed that the deposited resistive material is uniformly distributed on the surface of the resistor. Equations (1)–(3) represent modeling procedures of the sheet resistance for applying to EM simulations. R denotes the sheet resistance; ρ is the resistivity; σ is the conductivity; l is the length of the resistor in millimeters; and S and r are the cross-sectional area and radius in millimeters of the rod resistor, respectively. The calculated conductivity of the resistor is 25.46 S/m

$$R = \rho\frac{l}{S} = \rho\frac{l}{\pi r^2} = \frac{l}{\sigma\pi r^2} \tag{1}$$

$$\sigma = \frac{l}{R\pi r^2} \quad [\text{in S/mm}] \tag{2}$$

$$\sigma = \frac{1000l}{R\pi r^2} \quad [\text{in S/m}]. \tag{3}$$

B. Log-Scaled Coaxial Structure With a Distributed Ceramic-Carbon-Rod Resistor

Required parameters for constructing the log-scaled coaxial line are extracted using the following equations:

$$C = \frac{2\pi\varepsilon}{\ln(D/d)} \tag{4}$$

$$L = \frac{\mu_0\mu_r}{2\pi}\ln(D/d) \tag{5}$$

$$Z = \sqrt{\frac{L}{C}} = \frac{1}{2\pi}\sqrt{\frac{\mu_0\mu_r}{\varepsilon_0\varepsilon_r}}\ln(D/d) = \frac{138}{\sqrt{\varepsilon_r}}\ln(D/d) \tag{6}$$

$$D = d\exp\left(\frac{Z\sqrt{\varepsilon_r}}{138}\right) \tag{7}$$

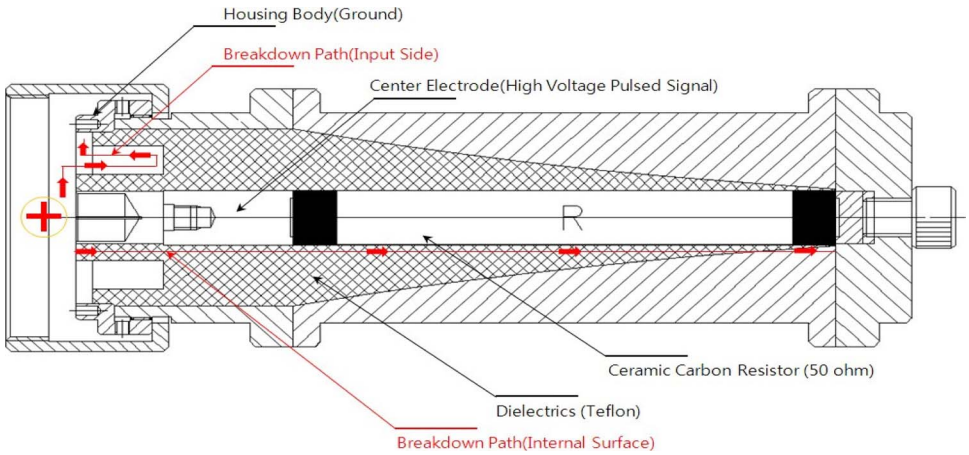

Fig. 5. Log-scaled coaxial structure with a 100-mm ceramic-carbon-rod resistor.

where C and L denote the capacitance and inductance of the coaxial line, respectively; Z is the characteristic impedance; and D and d are the outer diameters of the dielectrics and the center conductor, respectively. We used a rod resistor of which the diameter is 10 mm and the length is 100 mm. With fixing an inner diameter of the center electrode with 10 mm, the outer diameter in the coaxial line could be extracted by changing the parameter of Z from 0 to 50 Ω. At the position of the junction between the transition electrode and the resistor, coaxial impedance has to be constructed having impedance of 50 Ω and be gradually decreasing until reaching the impedance of 0 Ω within the finite length of 100 mm, as shown in Fig. 4.

Geometry of the log-scaled coaxial line with the calculated parameters is depicted in Fig. 5. A corrugated dielectric structure of the folded shape at the connector area extending the surface propagation length from the center conductor to its housing bodies provides a better high-voltage insulation performance. When using dielectrics as an insulation material, the pulsed breakdown is occurred along the dielectric's surface. For instance, air medium has a breakdown voltage about 3 kV/mm. Depending on the dielectric material, breakdown voltage goes to tens of kilovolts per millimeter. By the way, the conjunction area for assembling a rod-type resistor in the log-scaled coaxial geometry should be designed to resist for the input pulses having amplitudes over several tens of kilovolts. Folded structure can be one of the best solutions under a constraint of the finite space. When attaching an end of the resistor to the center conductor, diameters of the conjunction faces should not be changed in order to avoid impedance mismatching. We used copper cottons at the contact faces and tighten a resistor to the center conductor by an external screw.

C. High-Voltage Insulation

A difficulty for the high-voltage UWB termination load development is how we can determine a size of the resistive element between insulation and frequency performances. Although physically and electrically long resistors give enough insulation performance to prevent a breakdown phenomenon, they do not operate as the lumped parameters. It means that the electrically long resistor has limited frequency performance. In the aspect of the high-voltage insulation, the weakest point is the conjunction face of connectors (see the breakdown path depicted with arrows in Fig. 5) because there is the shortest propagation path of an electrical breakdown between the signal line and the ground. Normally, dielectric material has a strong insulation property exceeding tens of kilovolts. Insulation problems normally happened at the conjunction faces of the discontinuous dielectrics (see folded dielectrics in Fig. 5) filling with air. Although air is normally a good insulator, it becomes partially conductive when stressed by a pulsed voltage having enough electric field strength.

Consistent pulsed power can culminate the complete electrical breakdown forming an electrical spark or arc that bridges the entire gap. Surface propagation length for preventing an air breakdown has to be calculated. Corrugating structure of the conjunction faces of connectors provides the longer dielectric surface propagation length under the restrictions of the finite outer diameter in the coaxial geometry, as shown in Fig. 5. The designed load device has an insulation performance operating up to 132 kV.

D. EM Simulation Analysis

The proposed log-scaled coaxial termination load is designed and analyzed in the time and frequency domains using CST Microwave Studio. When inserting a 100-mm rod resistor into the nonscaled coaxial transmission line, as shown in Fig. 8, the synthetic impedance is varying at every positions of the load device, as depicted in Fig. 6. Results of a TDR and S-parameters according to changing a diameter of dielectrics (Polytetrafluoroethylene (PTFE), permittivity 2.2) from 20 to 40 mm with the step of 4 mm are represented in Figs. 6 and 7. The distributed ceramic-carbon-rod resistor having a diameter of 10 mm and a length of 100 mm is used as a center conductor. As a reference, the TDR result when using a center conductor of a brass electrode having same dimensions with the rod resistor is plotted in Fig. 6. Horizontal time axis denotes a distance along the resistor with the propagation velocity of 20.225 cm/ns. As we expected, synthetic coaxial impedance is varying from 30 to 100 Ω in 10-cm distance.

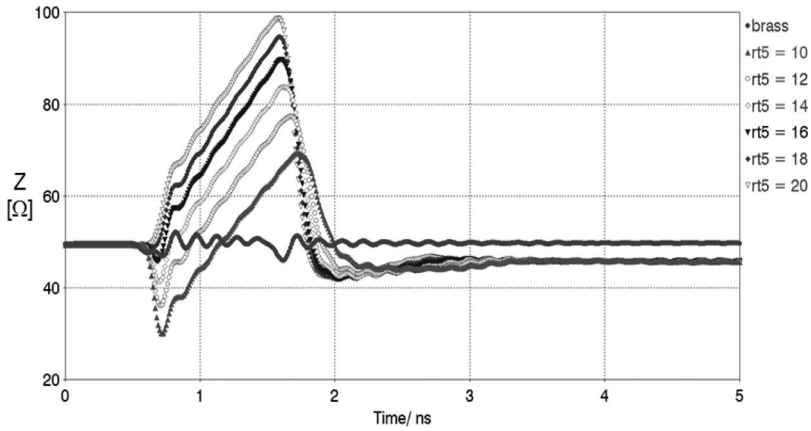

Fig. 6. TDR analysis with changing outer diameters of a coaxial line from 20 to 40 mm with a step of 4 mm (rt5 is a radius of dielectrics in a coaxial geometry).

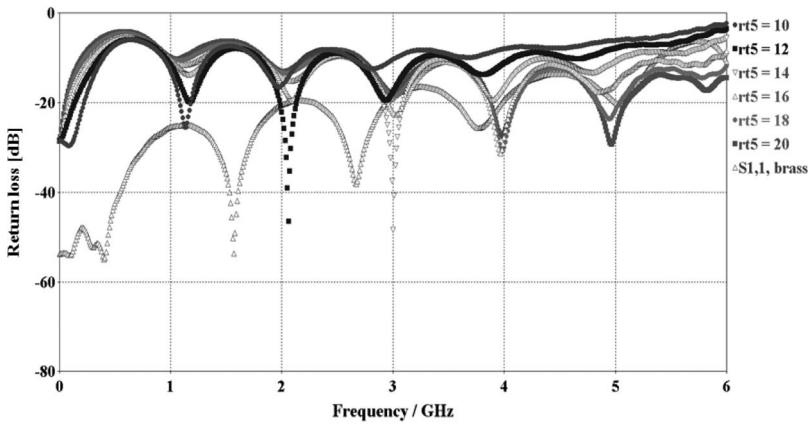

Fig. 7. S-parameter analysis for varying an outer diameter of a coaxial line from 20 to 40 mm with a step of 4 mm (rt5 is a radius of dielectrics in a coaxial geometry).

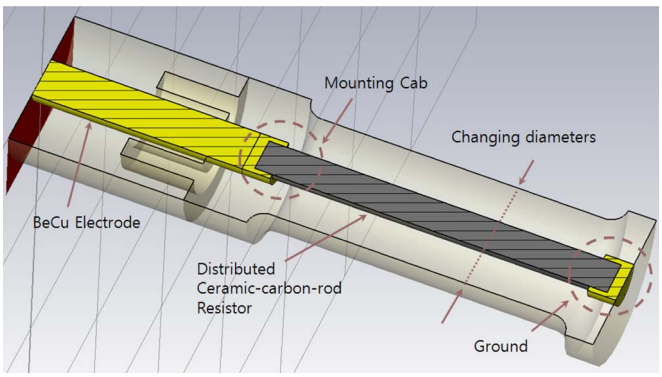

Fig. 8. Cross-sectional view of a nonscaled coaxial simulation model with changing diameters of dielectrics. Parameter "rt5" in Figs. 6 and 7 denotes a radius of dielectrics in a coaxial geometry.

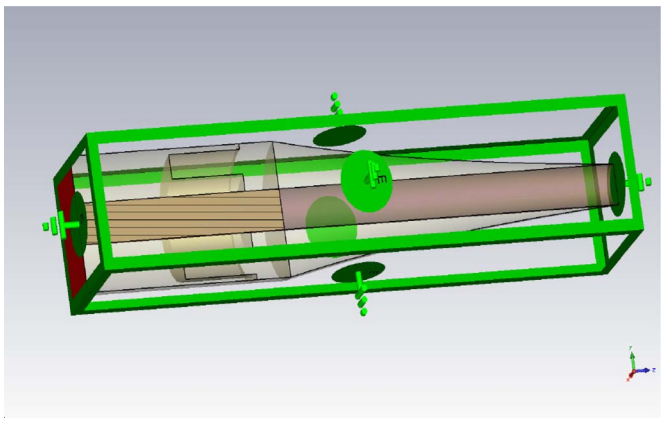

Fig. 9. Log-scaled coaxial load modeling in CST Microwave Studio.

One more thing that should be carefully designed is the conjunction face of a metallic electrode and the rod resistor.

In Fig. 7, the case using a brass electrode instead of the rod resistor shows that mismatching occurs at frequencies beyond 3 GHz. It is caused by a mounting cab on the location of conjunction faces between the BeCu electrode and the rod resistor (see Fig. 8). Matching performance is getting worse and worse as the frequency goes higher due to the impedance discontinuity at the mounting cab. In the holding structure of the mounting cab, the ratio of the coaxial diameter is changed so that the coaxial impedance is not maintained at this point. When designing the proposed log-scaled coaxial load, this fact is considered and designed to have a direct facing structure without any holding cabs at the conjunction faces, as shown in Fig. 9. The load device is composed of inner BeCu electrodes, enclosing PTFE dielectrics, a resistive

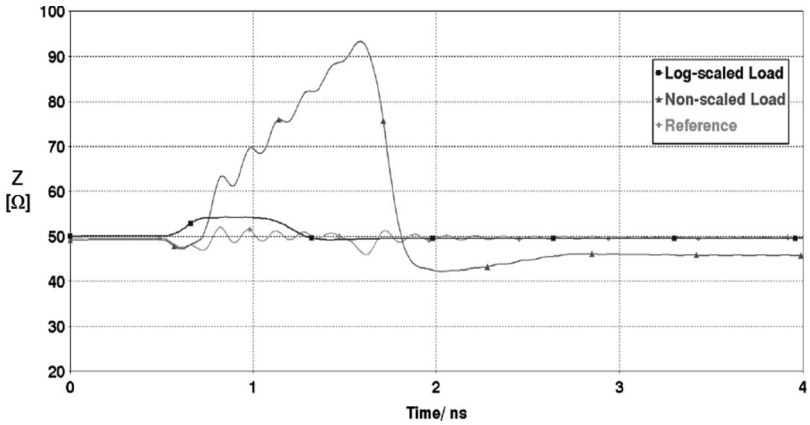

Fig. 10. TDR impedance analysis: Comparison of impedance for a normal case, a nonscaled case, and a log-scaled case.

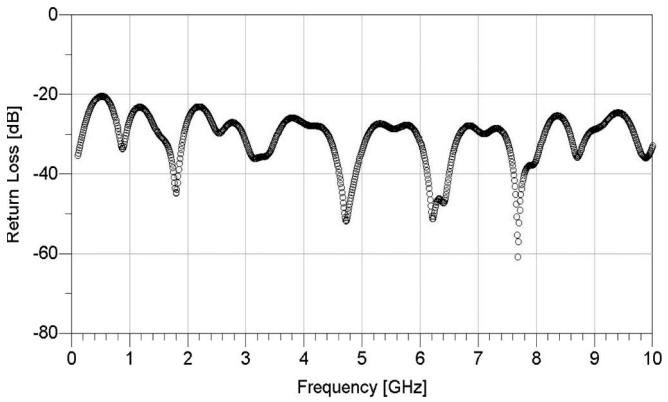

Fig. 11. Simulated return loss of the proposed log-scaled coaxial load using a 100-mm distributed ceramic-carbon-rod resistor.

solid rod, and an outer metal housing, as represented in Fig. 5. The outer housing metal was modeled as a perfect electric conductor for saving analysis time. For the dielectrics, PTFE was chosen having a dielectric constant of 2.2. For the resistive solid rod, the commercial carbon-rod resistor of R1005A051J, produced by HVR Company Ltd., is used. BeCu electrodes were used for inner metal electrodes. TDR and S-parameter analysis were performed to estimate impedance variations in percent values and matching performance in the frequency range of 0.1–10 GHz, respectively. Simulated results are shown in Figs. 10 and 11. In Fig. 10, the reference plot means a normal coaxial geometry that a metal electrode is used as a center conductor in the nonscaled coaxial structure. The nonscaled structure represents a case that the carbon-rod resistor is used at the position of the center conductor. A log-scaled structure denotes an impedance-compensated case for the nonscaled structure by means of diminishing the coaxial characteristic impedance. A log-scaled coaxial case provides a notable improvement in the aspect of the impedance variation. Matching performance was improved with ten times better than the nonscaled one.

Fig. 11 shows a simulation result of the impedance matching performance in the frequency domain achieving return loss below -20 dB up to 10 GHz. It means that a reflected power value is only below 1% with respect to the incident signal power.

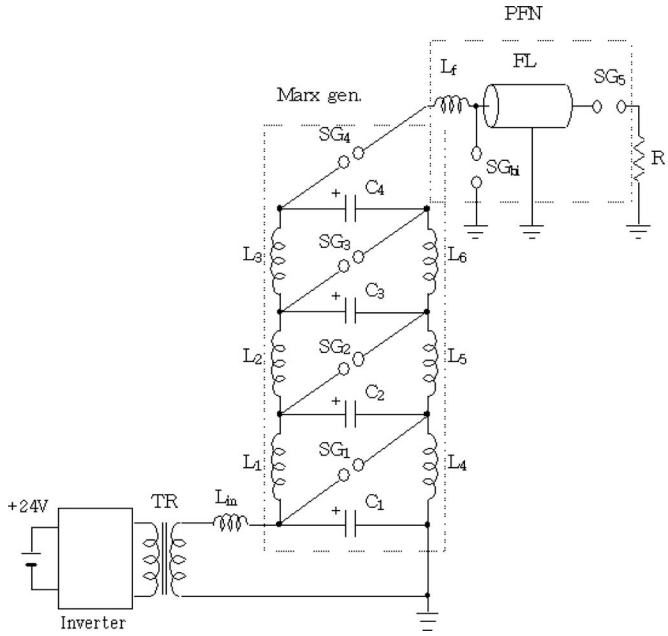

Fig. 12. Circuit diagram of a laboratory-developed UWB pulse generator.

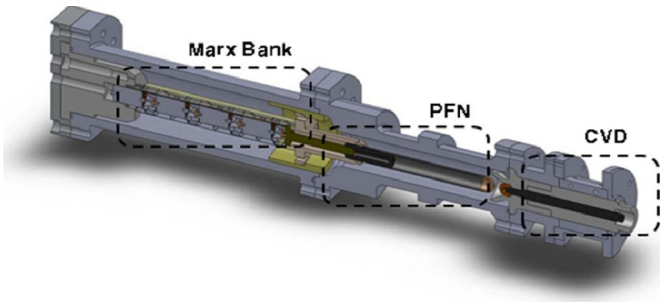

Fig. 13. Three-dimensional CAD model of the Marx generator and PFN structure in a laboratory-developed UWB pulse generator. The Marx generator is composed of four-stage parallel capacitors, each having a charging voltage rate of 50 kV.

IV. Experimental Setup

A. High-Voltage UWB Pulse Generator

A Marx generator-driven LC resonant spark-gap pulse generator was designed and implemented for testing a termination

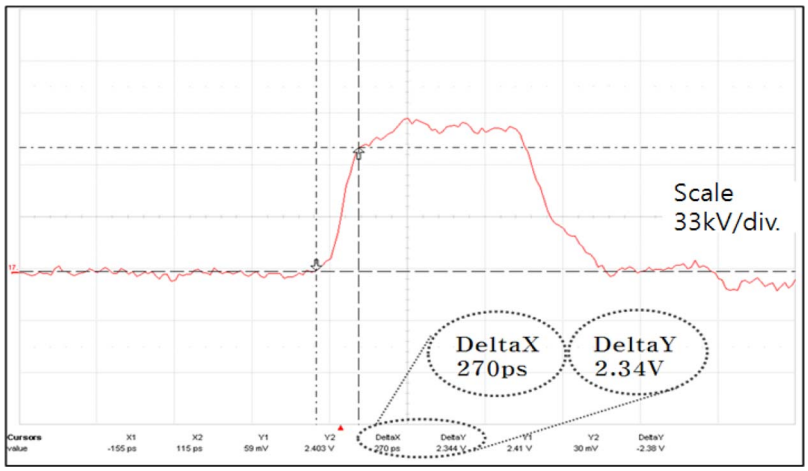

Fig. 14. Output pulse waveform of a laboratory-developed UWB pulse generator: Peak amplitudes of 90 kV and a rise time of 270 ps with nitrogen gas of 17 bars.

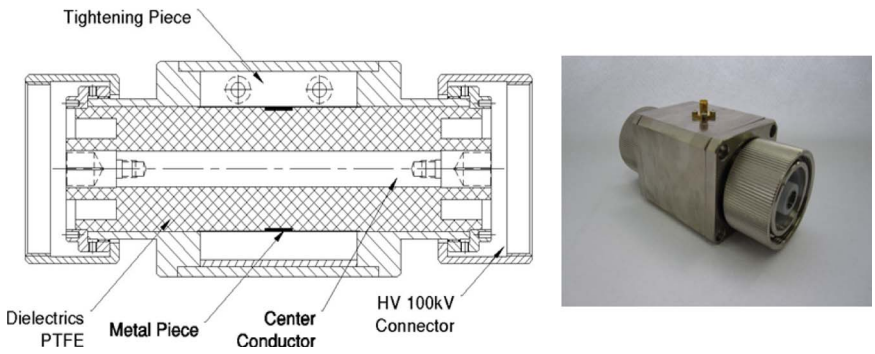

Fig. 15. CVD: Cross-sectional view in (left) a CAD drawing and (right) implemented photograph.

performance with respect to high-voltage fast transient pulse signals. Fig. 12 shows a circuit diagram of the pulse generator. It consists of a primary power supply with a battery (24 VDC/ 4AH), an inverter circuit, a high-voltage transformer, a four-stage Marx generator with spark-gap switches between each capacitor's ends, and a pulse forming line for shaping a pulse with a rise time below 1 ns. The inverter circuit generates high-frequency (several hundreds of kilohertz) pulse-modulated signals from the battery. Capacitors in the Marx generator are charged by the LC resonant circuit until reaching at its maximum charged voltage, and then break down through the connected spark-gap switches in a short time. A pulse compression is occurred at the final stage of the pulse forming network (PFN). A rise time of an output pulse is under 300 ps. The Marx capacitor bank is charged up to 200 kV in the open-load condition when spark-gap switches of SG1–SG3 are all closed. In the matched condition, a 100-kV voltage pulse can be achieved at the load. The implemented Marx generator and PFN with a CVD are shown in Fig. 13. Fig. 14 shows the output pulse waveform of the laboratory-developed UWB pulse generator, implemented by HVP Inc. in Korea. An FWHM pulsewidth is about 1.2 ns, which is relatively long compared to its rise time.

The developed pulse generator uses nitrogen (N_2) gas for tuning the output pulse amplitude with the rise time. Gas pressure range is from 10 to 20 bars. The output pulse in Fig. 14 was plotted when the gas pressure is 17 bars. A peak voltage is about 90 kV with the rise time of 270 ps. At 20 bars, amplitudes of pulse go to above 100 kV with the rise time of 250 ps. It can also generate bipolar pulses by tuning an external electrode (SGbi). The amplitude of bipolar pulse is about 150 kVpp.

B. CVD

A high-voltage fast transient pulse signal cannot be measured with a wideband oscilloscope directly due to the dynamic range limit. A possible voltage range of an oscilloscope that operates with gigahertz bandwidth is limited within several volts. High-voltage wideband pulse attenuators could be necessary, but it is very expensive and complicated to design. A CVD is the one of good candidates to measure a high-voltage fast transient pulse signal in low cost. Additive parasitic capacitance between the center conductor and the ground is created by inserting a metal piece into a coaxial line nearby the inner surface of an outer conductor, which is separated by the dielectric film. Dielectric film is formed with a layer of thin synthetic plastic films such as Mylar over a flat electrode surface. It can provide a capacitance value to ground of about 2–20 nF. The layer of Mylar can be fastened to the flat surface of the electrode using a special adhesive and metal piece of copper foil. The thickness of Mylar films required for making such high capacitance values is a few micrometers. A cross-sectional view of CVD construction on the coaxial transmission line is depicted in Fig. 15. A tightening piece is for maximizing a division ratio by minimizing a gap distance. Calibration of the CVD was

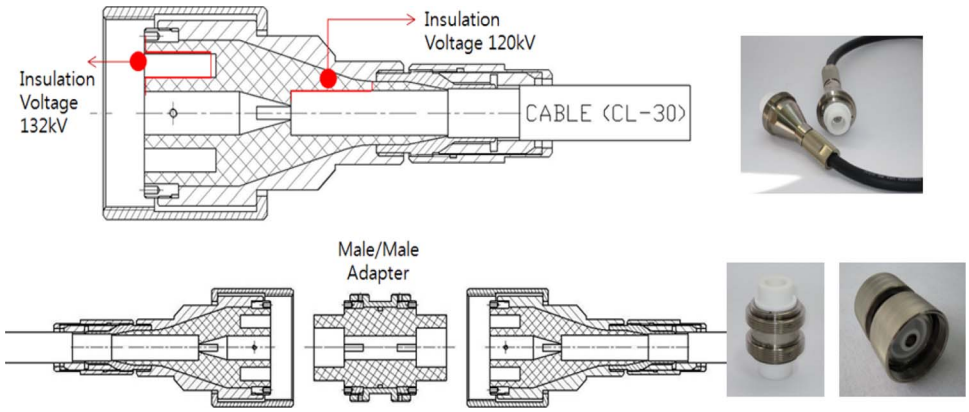

Fig. 16. Assembly configurations of cable connectors and adaptors.

Fig. 17. Assembled photograph of the proposed log-scaled load device.

performed using a commercial pulse generator of FPG 20-P, manufactured by FID GmbH in Germany. The implemented CVD device shows the division ratio of 1/330 having amplitude up to 100 kV with the rise time below 300 ps. A division ratio of the CVD was evaluated by comparing the division pulse voltage of the CVD with attenuated values using the commercial high-voltage pulse attenuators, as shown in Fig. 22.

C. High-Voltage Connectors and Adaptors

Configuring measurement setup for a log-scaled coaxial load device requires customized connectors and transition adaptors for evaluating termination performances with respect to high-voltage subnanosecond pulse signals. Fig. 16 shows assembly drawings and pictures for the high-voltage cable connectors and adaptors. Interface of connectors and adaptors was designed satisfying 50-Ω coaxial impedance and the insulation performance over 100 kV, i.e., same with the proposed log-scaled load device (see Fig. 17). A grooved structure on the dielectric surface of connectors and adaptors also provides a convenient feature to change from female geometry to male one by fitting a grooved hole with a dielectric ring and a piece of internal electrode. Cable connectors are configured to allow the core of the high-voltage coaxial cable to be coupled with the inner electrode of the connector in a threaded manner so that assembling and disassembling are easier rather than soldering way. An insertion loss of a fabricated high-voltage cable assembled with connectors at both ends is measured with 0.45 dB/m at 1 GHz, and return loss is below -20 dB from 40 MHz to 10 GHz.

D. Measurement Setup

Measurement setup for a high-voltage impulse termination is shown in Fig. 18. A pulse generator is made up of two different types of sources. One is a commercial semiconductor switch-based pulse generator, FPG 20-P, and the other is a laboratory-developed spark-gap switch-based UWB pulse generator. TDR results with FPG 20-P would provide operation frequency validity up to 10 GHz for the proposed load device, but it cannot show the voltage insulation capability up to 100 kV because the maximum output voltage is limited less than 20 kV. The developed UWB pulse generator can give a validity of the high-voltage insulation performance up to 100 kV but cannot give any information of its frequency usage up to 10 GHz, vice versa. Table I represents electrical specifications of two test sources in detail.

FPG 20-P shows an amplitude of < 20 kV, a rise time of < 150 ps, and repetition rates of < 10 kHz. The laboratory-developed UWB source shows an amplitude of < 100 kV, a rise time of < 300 ps, and repetition rates of < 100 Hz. Both two sources have an output impedance value of 50 Ω.

In Fig. 18, an in-house developed high-voltage coaxial cable assembled with connectors connects the output of a pulse generator to the input of the CVD device. The division port of the CVD is connected to 40-dB pulse attenuators, manufactured in Barth Electronics Inc., and the output port of the CVD is linked to the input of the proposed coaxial load device through a 100-kV male-to-male adaptor. Scaling factor of an oscilloscope is 1/33 000 since the division ratio of the CVD is about 1/330. Small-signal test setup is not explained in detail, but a vector network analyzer of 37347C, manufactured in Anritsu Corporation, is used with in-house developed cable-type adaptors transforming from a 100-kV interface to an n-type interface.

V. Experimental Results

A. UWB Frequency Performance

The small-signal network performance of an impedance matching property is measured from 40 MHz to 10 GHz, as shown in Fig. 19. Return loss is below -20 dB in the entire test frequency band. The solid line represents a measured return loss plot of the proposed log-scaled load device, and the dotted line denotes a simulated result in CST Microwave Studio.

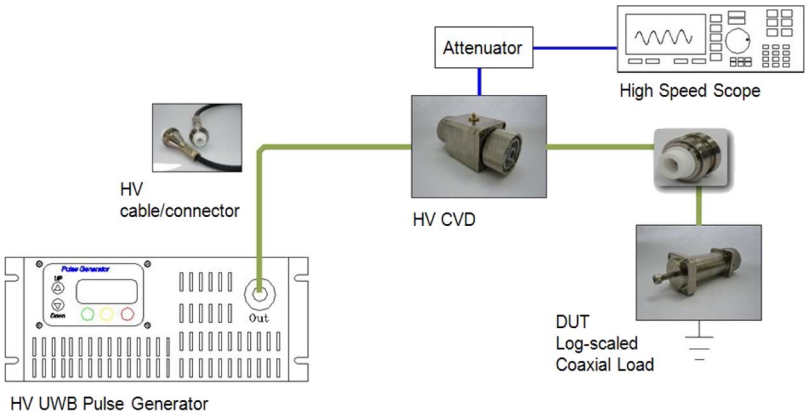

Fig. 18. Test configurations of termination performance of a load device for high-voltage fast transient pulses using the CVD and load.

TABLE I
SPECIFICATIONS OF TWO DIFFERENT TYPES OF UWB PULSE GENERATORS

Items	FPG 20-P	Developed UWB Source
Waveform	Gauss exponential	Bell-shape
Peak amplitude	15 - 20kV	50 - 100 kV
Rise time	100 - 150 ps	250 - 300 ps
FWHM[a]	1 ns	1.4 ns
Impedance	50 ohm	50 ohm
Repetition frequency	< 10 kHz	< 100 Hz

[a]FWHM is abbreviation for Full Width at Half Maximum amplitude.

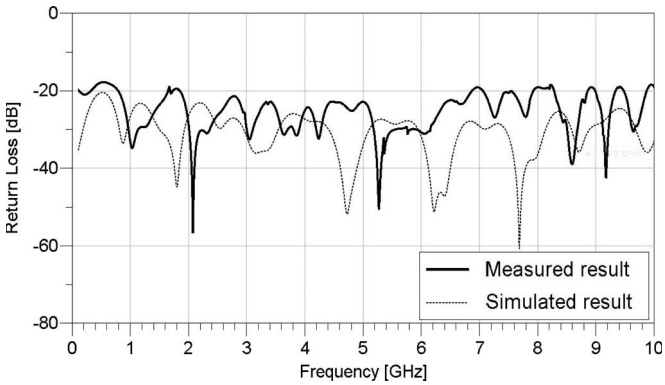

Fig. 19. Return loss plot of the proposed log-scaled load device: (dotted line) simulated result and (solid line) measured result.

Measured performance is well coincident with the simulated results except frequencies above 6 GHz. It might be caused by the cable-type conversion adaptors having similar S11 trajectory in Fig. 19.

Fig. 20 shows a comparison of a measured return loss between the nonscaled and proposed log-scaled structures. Return loss is notably enhanced in the entire test frequency band. As aforementioned, the nonscaled load device does not operate as a proper termination device and may cause serious errors in the analysis data. Matched impedance property may be expressed with a TDR analysis in the time domain.

We used a TDR scope, a model of TDS520, produced by Tektronix.

A pulse generator in the TDR equipment generates a fast transient impulse with a rise time of 20 ps, and its output

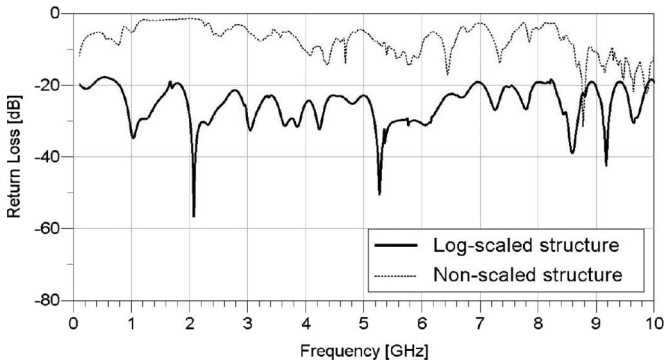

Fig. 20. Measured return loss plots of two types of a load device: (dotted line) nonscaled structure and (solid line) log-scaled structure.

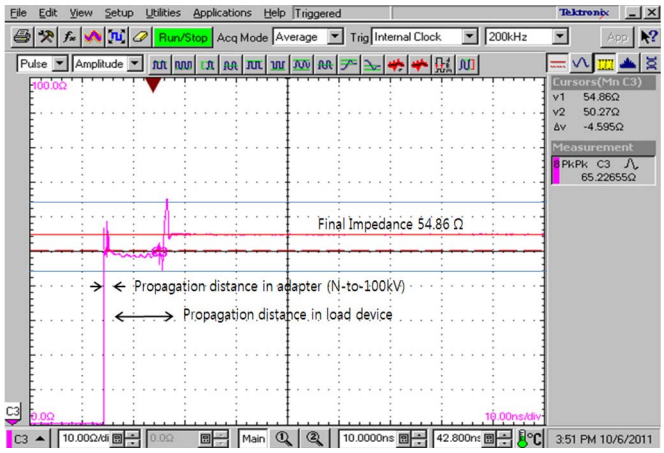

Fig. 21. Measured TDR plot for the proposed log-scaled load device.

impedance is 50 Ω. Fig. 21 represents a measured TDR performance of the log-scaled load device.

In the TDR plot, impedance is finally converged to 54.86 Ω after passing through the log-scaled coaxial load device. Fluctuations of the impedance might be caused by discontinued conjunction faces in the adaptor and components of the load device. The reason we analyzed that impedance peaking is caused by the discontinuity in the load device is the fact that the location of the peak value is coincident with conjunction surfaces between the transition electrode and the carbon resistor, as shown in Fig. 5. Results of S-parameter and TDR analysis imply that the proposed log-scaled structure is useful

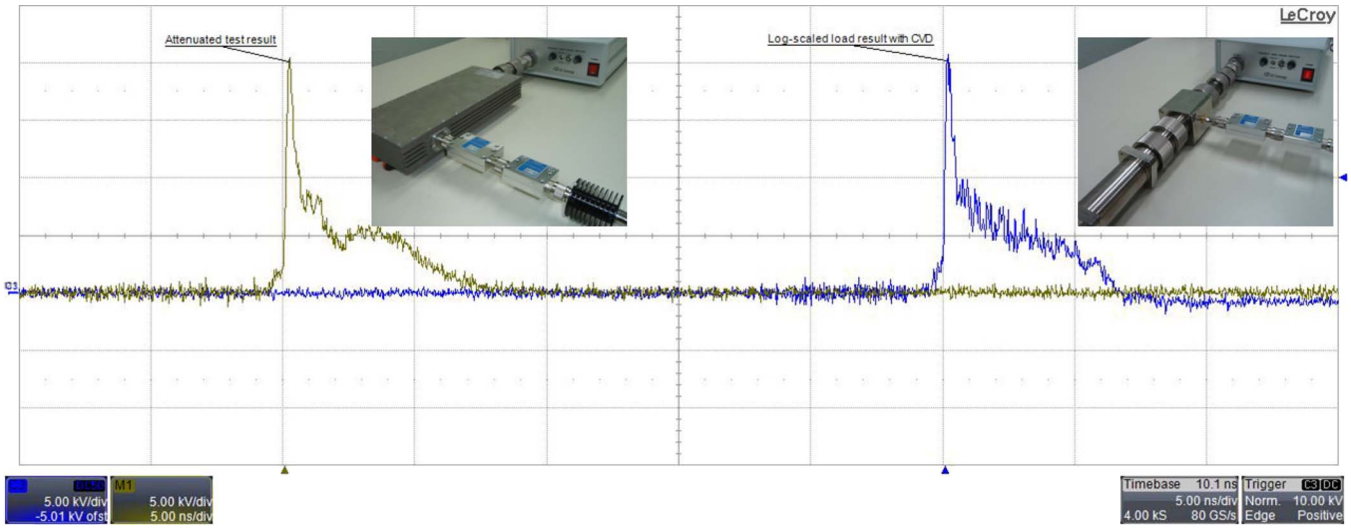

Fig. 22. Comparison of measured pulse waveforms between an attenuated case (see the left test setup) and a coupled case using a CVD with the log-scaled load (see the right test setup) applying output pulses of FPG 20-P in wide temporal span (5 ns/div.).

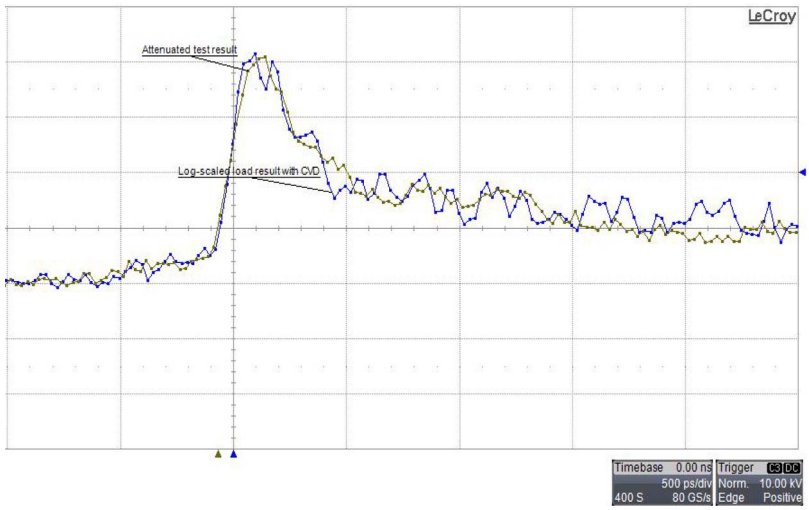

Fig. 23. Measured pulse waveforms of an attenuated case and a coupled case using a CVD with the log-scaled load in narrow temporal span (500 ps/div.).

for obtaining performances of high-voltage insulation and UWB frequency simultaneously even using an electrically long distributed resistor.

B. High-Voltage Pulse Termination Performance

A high-voltage repetitive pulse termination is evaluated using an experimental setup, as shown in Fig. 18. High-voltage operation is diagnosed by measuring reflected pulses at the division port of the CVD in the predictable time range of 15 ns when reflection occurs at the conjunction point of the CVD and the load device. In Fig. 18, a high-voltage coaxial cable with in-house implemented connectors is 1.2-m long and the length of the CVD device is about 10 cm. Measured reflected pulses are represented in Figs. 22 and 23. In Figs. 22 and 23, FPG 20-P was used as a test source. Two cases were benchmarked that one is a case of using commercial pulse attenuators (see the left picture of the test setup in Fig. 22) and the other is a case of using in-house developed CVD with the log-scaled load (see the right picture of the test setup in Fig. 22) device.

Additional two 20-dB attenuators of Barth Electronics Inc. are used in cascade at the division port of the CVD. Both cases represent almost the same waveforms in aspects of a rise time and peak voltage amplitudes. In addition, there are no reflection pulses after an incident pulse within 15 ns, which means that the attached load device to the CVD output provides excellent impedance matching performance with respect to a pulsed input in that of amplitudes up to 20 kV, a rise time below 150 ps, and repetition rates below 10 kHz. For investigating maximum operation voltage, a laboratory-developed UWB pulse generator was used in a test configuration in Fig. 18. Measured pulse waveform at the division port of the CVD with additional attenuation of 40 dB is plotted in Fig. 24.

An output pulse amplitude in Fig. 24 is about 114.5 kV, and a rise time is about 250 ps. Time and amplitude resolutions are 5 ns/div. and 100 V/div., respectively. Attenuators connected to the division port of the CVD are calibrated by setting offset values with 1/100 in an oscilloscope. As shown in Fig. 24, there are no reflected pulses within 25 ns after a time spot where a peak pulse is detected.

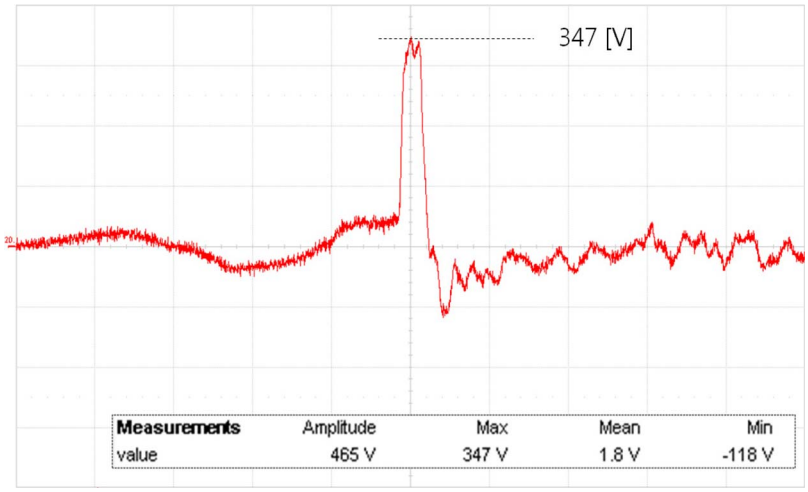

Fig. 24. Measured pulse waveforms using a CVD with the log-scaled load device applying a 114.5-kV pulse using a laboratory-developed UWB pulse generator in wide temporal span (5 ns/div.).

VI. Summary and Conclusion

In this paper, we have presented a design method and evaluation results of the log-scaled coaxial load device for terminating the high-voltage subnanosecond pulse signals using a 10-cm distributed ceramic-carbon-rod resistor. The physical length of a rod resistor is far longer than a wavelength of an input pulse so that impedance linearly increases in the moving direction of an incoming pulse. A proposed high-voltage UWB log-scaled coaxial load with a distributed ceramic-carbon-rod resistor has a property to compensate the varying impedance, which is caused by an electrically long rod resistor by means of diminishing the coaxial characteristic impedance exponentially along the resistor. Consequently, it can provide consistent impedance in the entire load device.

Experiments are performed with TDR and S-parameter analysis to verify small-signal wideband performance. For high voltage diagnostics verifying the high-voltage operation validity, commercial FPG 20-P and laboratory-developed UWB pulse generator are used. FPG 20-P has a performance of an amplitude of < 20 kV, a rise time of 100–150 ps, and repetition rates of $<$ 10 kHz. The laboratory-developed UWB pulse generator has output amplitudes of 100 kV at gas pressures of 20 bar, a variation range from 50 to 100 kV by controlling gas pressures, and a rise time of 250–300 ps with a maximal repetition frequency of 100 Hz.

The UWB capacitive voltage probe device (CVD), which has a division ratio of 1/330, is also implemented and used to measure a high-voltage pulse reflection in the time domain. Experimental results show good agreement with expectations for the voltage standing-wave ratio under $1.25:1$ from dc to 10 GHz, a peak impedance variation under 10%, and a stabilized value of 54.86 Ω with negligible reflections. An injected input pulse has amplitudes from 15 to 100 kV, a rise time below 1 ns, and repetition rates under 10 kHz. The proposed coaxial load device is adequate for terminating a high-voltage fast transient pulse signal of which the duty cycle is below 0.001% because of a capacity of heat dissipation of the rod resistor.

Acknowledgment

The authors would like to thank Dr. W.-H. Kim and HVP Inc. in Korea for cooperating and advising in the high-voltage pulse test.

References

[1] T. Weber, "Measurement techniques for conducted HPEM signals," *IEEE Trans. Electromagn. Compat.*, vol. 46, no. 3, pp. 431–438, Aug. 2004.
[2] M. Camp, "Susceptibility of personal computer systems to fast transient electromagnetic pulses," *IEEE Trans. Electromagn. Compat.*, vol. 48, no. 4, pp. 829–833, Nov. 2006.
[3] D. Nitsch, "Susceptibility of some electronic equipment to HPEM threats," *IEEE Trans. Electromagn. Compat.*, vol. 46, no. 3, pp. 380–389, Aug. 2004.
[4] M. Bäckström, "Susceptibility of electronic systems to high-power microwaves: Summary of test experience," *IEEE Trans. Electromagn. Compat.*, vol. 46, no. 3, pp. 396–403, Aug. 2004.
[5] D. Nitsch, "Prediction of ultra wide band coupling to modern electronic equipment," in *Proc. EMC*, Wroclaw, Poland, Jun. 2002, pp. 103–108.
[6] H. Akiyama, "Industrial applications of pulsed power technology," *IEEE Trans. Dielect. Elect. Insul.*, vol. 14, no. 5, pp. 1051–1064, Oct. 2007.
[7] Z. Fang, "Surface treatment of polyethylene terephthalate films using a microsecond pulse homogeneous dielectric barrier discharges in atmospheric air," *IEEE Trans. Plasma Sci.*, vol. 38, no. 7, pp. 1615–1623, Jul. 2010.
[8] M. Sira, "Surface modification of polyethylene and polypropylene in atmospheric pressure glow discharge," *J. Phys. D, Appl. Phys.*, vol. 38, no. 4, pp. 621–627, Feb. 2005.
[9] T. Tang, "Diode opening switch based nanosecond high voltage pulse generators for biological and medical applications," *IEEE Trans. Dielect. Elect. Insul.*, vol. 14, no. 4, pp. 878–883, Aug. 2007.
[10] A. Kuthi, "Nanosecond pulse generator using fast recovery diodes for cell electromanipulation," *IEEE Trans. Plasma Sci.*, vol. 33, no. 4, pp. 1192–1197, Aug. 2005.
[11] A. Pokryvailo, "A compact source of subgigawatt subnanosecond pulses," *IEEE Trans. Plasma Sci.*, vol. 32, no. 5, pp. 1909–1918, Oct. 2004.
[12] S. Lyubutin, "High-power ultrafast current switching by a silicon sharpener operating at an electric field close to the threshold of the Zener breakdown," *IEEE Trans. Plasma Sci.*, vol. 38, no. 10, pp. 2627–2632, Oct. 2010.
[13] L. Pecastaing, "Very fast rise-time short-pulse high-voltage generator," *IEEE Trans. Plasma Sci.*, vol. 34, no. 5, pp. 1822–1829, Oct. 2006.
[14] K. Liu, "A high repetition rate nanosecond pulsed power supply for nonthermal plasma generator," *IEEE Trans. Plasma Sci.*, vol. 33, no. 4, pp. 1182–1185, Aug. 2005.
[15] G. Mesyats, "The RADAN series of compact pulsed power generators and their applications," *Proc. IEEE*, vol. 92, no. 7, pp. 1166–1179, Jul. 2004.
[16] B. Cadilhon, "High pulsed power sources for broadband radiation," *IEEE Trans. Plasma Sci.*, vol. 38, no. 10, pp. 2593–2603, Oct. 2010.
[17] C. Spikings, "High performance attenuator," in *Proc. IEE Symp. Pulsed Power (Dig. 1999/030)*, 1999, pp. 15/1–15/6.

Seung-Kab Ryu was born in Seoul, Korea, in 1976. He received the B.S. degree in avionics in 1999 from Hankuk Aviation University, Goyang, Korea, and the M.S. degree in mechatronics in 2001 from Gwangju Institute of Science and Technology, Gwangju, Korea, where he is currently working toward the Ph.D. degree.

From 2001 to 2004, he was with Millitron Inc., as the Senior Engineering Staff for the development of millimeter-wave transceiver and outdoor unit development. He is currently with the Convergence Technology Department, Attached Institute of Electronics and Telecommunication Research Institute, Daejeon, Korea. His research interests are in the development of high-voltage plasma limiter for high-power microwave protection and subnanosecond pulsed-power source for intentional electromagnetic interference immunity research on microwave and wireless equipment pieces.

Yong-Hoon Kim (M'90) was born in Donghae, Korea, in 1952. He received the B.S. degree in radio science and engineering from Kyung Hee University, Seoul, Korea, in 1974; the M.S. degree in electronic engineering from Yonsei University, Seoul, in 1976; and the Dr.-Ing. degree from the University of Stuttgart, Stuttgart, Germany, in 1990.

From 1976 to 1980, he was an Instructor with the Second Air Force Academy in Korea. From 1990 to 1994, he was with Korea Aerospace Research Institute as the Department Head of Space Application Technology, Avionics, and Space Payload. Since 1995, he has been a Professor with the School of Information and Mechatronics, Gwangju Institute of Science and Technology, Gwangju, Korea. Since then, he has contributed to the development of microwaves, millimeter-wave components, millimeter-wave active and passive imaging systems, and high-speed millimeter-wave communication systems. He is currently focused on the medical application of radars, radiometers for noninvasive measurement, and millimeter-wave polarimetric image radiometers. He is also focused on CMOS one-chip SoC for laboratory-developed radar and radiometer systems. In 2000, he founded Millisys Inc., Gwangju, where has been a representative. As a result of outstanding research activities in his field, he holds several patents for method and apparatus for obtaining high-resolution images in Korea, the U.S., and Japan.

Dr. Kim is a Board Member of the Korean Society of Remote Sensing and the Korean Institute of Electromagnetic Engineering and Science.